Journal of Materials Chemistry

Cite this: *J. Mater. Chem.*, 2012, **22**, 5792

www.rsc.org/materials

PAPER

Imidazole-functionalized polymer microspheres and fibers – useful materials for immobilization of oxovanadium(IV) catalysts†

Ryan S. Walmsley, Adeniyi S. Ogunlaja, Matthew J. Coombes, Wadzanai Chidawanyika, Christian Litwinski, Nelson Torto, Tebello Nyokong and Zenixole R. Tshentu*

Received 27th October 2011, Accepted 3rd February 2012
DOI: 10.1039/c2jm15485d

Both polymer microspheres and microfibers containing the imidazole functionality have been prepared and used to immobilize oxovanadium(IV). The average diameters and BET surface areas of the microspheres were 322 μm and 155 $m^2 g^{-1}$ while the fibers were 1.85 μm and 52 $m^2 g^{-1}$, respectively. XPS and microanalysis confirmed the incorporation of imidazole and vanadium in the polymeric materials. The catalytic activity of both materials was evaluated using the hydrogen peroxide facilitated oxidation of thioanisole. The microspheres were applied in a typical laboratory batch reactor set-up and quantitative conversions (>99%) were obtained in under 240 min with turn-over frequencies ranging from 21.89 to 265.53 h^{-1}, depending on the quantity of catalyst and temperature. The microspherical catalysts also proved to be recyclable with no drop in activity being observed after three successive reactions. The vanadium functionalized fibers were applied in a *pseudo* continuous flow set-up. Factors influencing the overall conversion and product selectivity, including flow rate and catalyst quantity, were investigated. At flow rates of 1–4 mL h^{-1} near quantitative conversion was maintained over an extended period. Keeping the mass of catalyst constant (0.025 g) and varying the flow rate from 1–6 mL h^{-1} resulted in a shift in the formation of the oxidation product methyl phenyl sulfone from 60.1 to 18.6%.

1. Introduction

Vanadium-dependant haloperoxidases (VHPO's) are enzymes that are capable of catalyzing the oxidative halogenation of organic molecules in the presence of hydrogen peroxide (H_2O_2).[1] The activity of these enzymes, however, extends to that of general oxidation reactions for example, the oxidation of sulfides to sulfoxides.[2,3] The active site typically consists of a vanadium ion (usually as vanadate) bound to an imidazole group of a histidine residue (Fig. 1).[4,5] Several functional and structural model complexes of these enzymes which exhibit catalytic activity have been prepared,[6] many of which contain imidazole[7,8] or benzimidazole[9,10] based ligands. These model complexes have been shown to catalyze the H_2O_2-facilitated oxidation of a range of substrates including but not limited to alkenes, sulfides, alkanes and alcohols.[10–12] Aqueous H_2O_2 generates water as the only theoretical by-product and is relatively cheap to purchase, making it an environmentally friendly alternative to the widely used chromium and permanganate based oxidising agents.

Immobilization of these complexes onto solid supports offers the practical advantage of simplifying separation and recyclability. Polymer supports have been used effectively in this regard. In particular, the functionalization of chloromethylated polystyrene resins with a ligand, followed by reaction with the metal

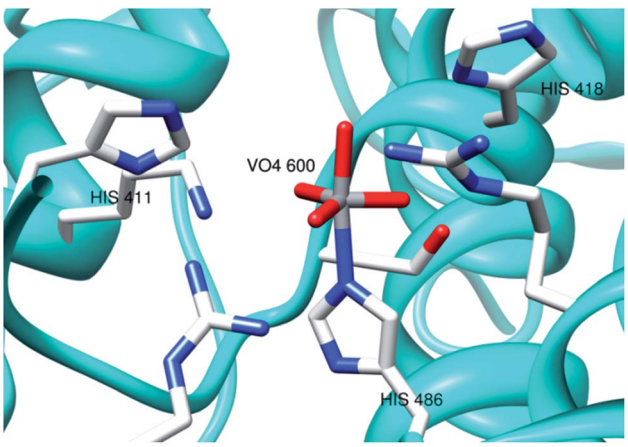

Fig. 1 The active site of the bromoperoxidase from *Ascophyllum nodusum* showing vanadium coordinated to the imidazole group of histidine residue (HIS 486) and the close proximity of two other histidine residues (HIS 418 and HIS 411).[4]

Department of Chemistry, Rhodes University, P.O. Box 94, Grahamstown, 6140, South Africa. E-mail: z.tshentu@ru.ac.za; Fax: +27 46622 5109; Tel: +27 46603 8846

† Electronic supplementary information (ESI) available: Additional photographs, synthesis, and catalysis results. See DOI: 10.1039/c2jm15485d

salt is a frequently applied strategy.[13,14] A related approach involves functionalization of the ligand with a polymerizable group, followed by suspension copolymerization with a suitable cross-linking agent. This method allows for a greater degree of freedom with respect to functional monomer (ligand) content, porosity, degree of cross-linking and bead diameter. The activity of these spherical heterogeneous catalysts may be improved by increasing the surface area-to-volume ratio. One way of doing this is to increase the pore structure within the beads, while another may be to reduce the diameter.[15] Unfortunately, as one decreases the size of the beads, they become difficult to separate and often require a centrifugation step.[16] In some instances this has been addressed by magnetizing the beads and separating them by application of an external magnetic field.[17]

Electrospinning is an emerging technique for obtaining high surface area-to-volume ratio polymer supports.[18] In electrospinning, a polymer solution or melt passes through a needle connected to a high voltage power supply. The charged solution experiences electrostatic repulsion at the needle tip until the surface tension is overcome, at which point the polymer jet accelerates towards a grounded collector. Electrospun fibers may have diameters in the micro to nano domain; but the entangled mat-like structure that forms makes separation very simple.[19] While the microspherical resins are often highly porous and hence may have comparatively larger surface areas than the fibers, it is questionable how accessible these pores are to substrates. Thus, it is likely that a large degree of catalysis takes place on the surface of the beads and since the fiber diameters are much smaller a greater degree of catalytic surface area is exposed.

Herein, we describe the preparation, characterization and catalytic activity of oxovanadium(IV) functionalized poly(vinylimidazole-*co*-ethyleneglycol dimethacrylate) microspheres produced by suspension polymerization. We have also prepared non-crosslinked poly(styrene-*co*-vinylimidazole) polymers by bulk polymerization which were subsequently electrospun into fibers and reacted with vanadyl sulfate to afford the corresponding oxovanadium(IV) immobilized fibers. The polymers were characterized by scanning electron microscopy (SEM), microanalysis, infrared (IR), X-ray photoelectron spectroscopy (XPS) as well as several other techniques. The activity of the catalysts was assessed by monitoring the oxidation of thioanisole in the presence of hydrogen peroxide, using gas chromatography (GC).

2. Experimental

2.1 Materials

Vinylimidazole (VIM, Sigma-Aldrich) was distilled under vacuum and kept at −20 °C. The comonomer styrene (ST, Sigma-Aldrich) and cross-linker ethylene glycol dimethacrylate (EGDMA, Sigma-Aldrich) were used as received. The radical initiator azobisisobutyronitrile (AIBN, Riedel de Haën) was recrystallized twice from methanol and dried under vacuum before use. Polyvinylalcohol ($M_w \sim 130\,000$, degree of hydrolysis 86.7–88.7 mol%) (PVA, Aldrich) was used as a stabilizing agent during suspension polymerization. Aqueous hydrogen peroxide was standardized by titration with potassium permanganate[20] and found to have an actual concentration of 29.4%. All other chemicals and solvents were purchased from commercial sources and used as received.

2.2 Instrumentation

The infrared spectra were recorded on either a Perkin Elmer 100 ATR-FTIR or Perkin Elmer 400 FT-IR spectrometer. The vanadium content was determined using a Thermo Electron (iCAP 6000 Series) inductively coupled plasma (ICP) spectrometer equipped with an OES detector. Wavelengths with minimum interferences were chosen (290.88 nm, 292.40 nm, 309.31 nm, 311.07 nm) and three repeats were performed at each wavelength. Progress of the catalysed reactions was monitored using the Agilent 7890A gas chromatograph (GC), fitted with a flame ionization detector (FID) and a Zebron, ZB-5MSi, capillary column (30 m × 0.25 mm × 0.25 μm). Mass spectra were obtained using a Thermo-Finnigan GC-MS fitted with an electron impact ionization mass selective detector. Microanalysis was carried out using a Vario Elementar Microcube ELIII. The polymer microspheres and fibers were imaged using a TESCAN Vega TS 5136LM scanning electron microscope (SEM). Atomic force microscopy (AFM) imaging was performed using a CP-11 Scanning Probe Microscope from Veeco Instruments (Carl Zeiss, South Africa) in non-contact mode at a scan rate of 2 Hz using a MP11123 cantilever. The AFM images were obtained using a spring contact (k) range of 20–80 N m^{-1} and resonant frequency (f_0) range of 217–276 kHz. X-ray photoelectron spectroscopy (XPS) measurements were performed with a Kratos Axis Ultra X-ray Photoelectron Spectrometer equipped with a monochromatic Al Kα source (1486.6 eV). The base pressure of the system was below 3×10^{-7} Pa. XPS experiments were recorded with 75 W power source using hybrid-slot spectral acquisition mode and an angular acceptance angle of ±20°. XPS data analysis was performed with Kratos version 2 program. Nitrogen adsorption/desorption isotherms were measured at 77 K using a Micromeritics ASAP 2020 Surface Area and Porosity Analyzer. Prior to each measurement, samples were degassed at 90 °C (fibers) and 150 °C (beads) for seven days. The surface BET area, total pore volume and pore size distribution were calculated from these isotherms.

2.3 Preparation of oxovanadium(IV) immobilized microspheres

p(VIM-*co*-EGDMA) microspheres. The functional monomer VIM (2 g), cross-linker EGDMA (7 ml) and initiator AIBN (0.15 g) were stirred in an organic phase consisting of a toluene/cyclohexanol (7 ml/2 ml) mixture (Scheme 1). In a separate 250 ml round bottom flask, an aqueous phase containing PVA (0.28 g) and NaCl (0.7 g) in 80 ml of water was stirred at 300 rpm. This solution was warmed to 60 °C to facilitate the dissolution of PVA. The organic phase was added dropwise to the aqueous phase under constant stirring. The temperature was increased to 70 °C and the reaction was allowed to proceed for 24 h under an argon atmosphere. The mixture was left to cool to room temperature and the beads were collected by filtration, washed several times with hot water followed by hot methanol and then dried in an oven at 60 °C overnight. These beads were then sieved and only the larger beads were retained (<25 mesh). Anal. Found: C, 59.95%; H, 7.80%; N, 6.52%.

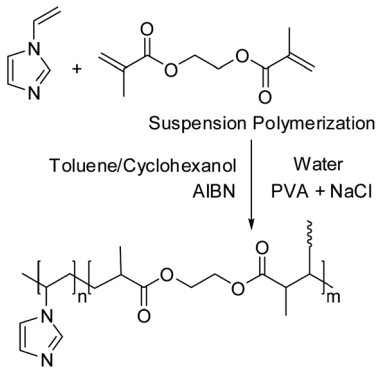

Scheme 1 Synthesis scheme for the preparation of p(VIM-*co*-EGDMA) microspheres.

p(VIM-*co*-EGDMA)-VO microspheres. 2.00 g of the <25 mesh size p(VIM-*co*-EGDMA) beads were swollen in 20ml of DMF for 2 h. To this was added excess $VOSO_4$ (1 g, 4.6 mmol) in DMF (50 ml). The mixture was heated to 60 °C and stirred overnight. The resultant blue-green beads were filtered and washed several times with DMF, water, methanol and finally diethyl ether and dried in an oven at 60 °C overnight. Anal. Found: C, 47.50%; H, 6.78%; N, 5.74%; S, 1.98%; V, 2.80%.

2.4 General procedure for copolymer preparation and fabrication of electrospun fibers

p(ST-*co*-VIM). In a typical reaction, VIM (1.6 g, 17.0 mmol) was mixed with styrene (6.4 g, 61.4 mmol) followed by addition of AIBN (0.2 wt%) (Scheme 2). The vial was sealed, purged with argon and the temperature increased to 60 °C. The reaction was allowed to proceed at this temperature for 48 h. The resultant solid polymer was subsequently dissolved in warm chloroform and precipitated by addition of methanol. This precipitation process was repeated twice to ensure removal of unreacted monomers. The white polymer was dried in an oven for 48 h at 60 °C. Anal. Found: C, 89.79%; H, 8.41%; N, 2.30%.

p(ST-*co*-VIM) fibers. The polymer was dissolved in a DMF/THF (4 : 1) solvent mixture to make a 25% solution (wt/v%). The polymer solution was stirred for 24 h to ensure complete dissolution and then loaded into a 20 ml syringe (Fig. 2). Electrospinning was then conducted using the following parameters. A voltage of 21 kV was applied to the spinneret (needle tip) which had an internal diameter of 1 mm, and the distance between the tip and collector was maintained at 20 cm whilst the flow rate was maintained at 1 ml h^{-1} using a syringe pump. The resultant white fibers were collected on a grounded piece of aluminium foil.

p(ST-*co*-VIM)-VO fibers. A strip of approximately 5 cm × 12 cm of the p(ST-*co*-VIM) fiber mat was cut and rinsed with water to make the fibers more manageable. These were placed into a 0.1 M $VOSO_4$ solution (20 ml methanol/5 ml water) in a sealable beaker. The vessel was purged with argon and then stirred gently at 120 rpm on an orbital shaker for a period of 72 h at room temperature. The fibers were rinsed with water and soaked in methanol for 3 h and then filtered. This procedure was repeated until no trace of vanadium was detected in the washings. Finally, the fibers were filtered and dried at room temperature under reduced pressure for 12 h. Anal. Found: C, 75.69%; H, 7.57%; N, 1.88%; S, 0.88%; V, 3.50%.

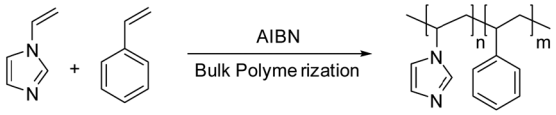

Scheme 2 Synthesis scheme for the preparation of the p(ST-*co*-VIM) copolymer.

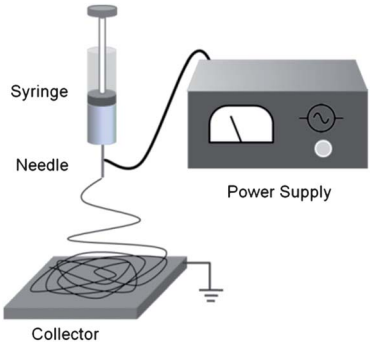

Fig. 2 Illustration of the electrospinning apparatus.

2.5 Catalytic activity studies

Catalytic activity of oxovanadium(IV) microspheres. In a typical reaction using the p(VIM-*co*-EGDMA)-VO microspheres; 20 ml of acetonitrile was added to a 100 ml round bottom flask fitted with a glass condenser and placed in an oil bath. The temperature of the oil bath was regulated to ±1 °C by using an external temperature probe. The stirring speed was kept constant at 300 rpm for all reactions. Thioanisole (1.24 g, 10 mmol) was then added followed by the required moles of aqueous H_2O_2. Following this immediately, the catalyst beads were added and this was considered the start of the reaction.

Catalytic activity of oxovanadium(IV) fibers. A required mass of vanadyl immobilized fibers were tightly packed in a 10 ml syringe, between two filter disks (Whatman No. 1) giving a catalyst bed with a diameter of approximately 11.5 mm and thickness ranging between 1–3 mm, depending on the mass of fibers used. In a separate vial, aqueous H_2O_2 (2 mmol) was added to thioanisole (0.124 g, 1 mmol) in methanol (10 ml). Methanol, rather than acetonitrile was used in this case since the non-crosslinked polymer fibers were partially soluble in acetonitrile. This solution, hereafter referred to as the reactant solution, was stirred for 5 min and then transferred to a 10 ml syringe. The reactant solution was then passed through the catalyst bed at a controlled rate, using a syringe pump. Fractions were collected in 1 ml portions and analysed by GC (Fig. 3).

3. Results and discussion

3.1 Synthesis and characterization of poly(VIM-*co*-EGDMA) microspheres

Microspherical poly(VIM-*co*-EGDMA) beads were successfully prepared by suspension polymerization using a similar method to

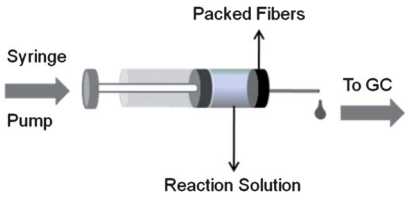

Fig. 3 An illustration of the continuous flow set up used in this study.

that reported by Uğuzdoğan *et al.*[21] We, however, found it necessary to include toluene as a co-solvent when using NaCl and PVA as stabilizers in the aqueous phase. The corresponding vanadyl-functionalized beads were prepared by reacting these imidazole-containing beads with vanadyl sulfate. The average diameter of the p(VIM-*co*-EGDMA) and p(VIM-*co*-EGDMA)-VO beads as determined by SEM was 313 and 322 μm respectively (n = 25). In addition, SEM showed that the p(VIM-*co*-EGDMA)-VO beads were spherical with a rough surface and a diameter distribution range of 251–408 μm (Fig. 4). As shown in AFM images (Fig. 5) there was a definite change of the surface morphology of the beads after functionalizing with vanadyl sulfate, going from a bumpy to a more ordered, plate-like morphology. After subjecting the p(VIM-*co*-EGDMA)-VO beads to a catalytic reaction, the surface structure changed only very slightly and in comparison to our previous work using chloromethylated polystyrene based microspheres (crosslinked with 5% divinylbenzene)[22] there was far less deterioration, possibly due to the higher amount of crosslinker used in this study. The surface roughness (Ra) of the p(VIM-*co*-EGDMA) beads decreased from 41.64 nm to 21.01 nm after reacting them with vanadyl sulfate. This trend has been observed in our previous work,[22] and may be due to the formation of a vanadyl coating on the surface.

The nitrogen content of the p(VIM-*co*-EGDMA) microspheres, which relates directly to the imidazole content as determined by microanalysis was found to be 6.52%, which translates to an imidazole/EGDMA ratio of roughly 2 : 3. In the infrared spectrum, an intense band appeared at 1719 cm^{-1} corresponding to the ν(C═O) from EGDMA, while imidazolyl group stretches were found at 1450, 1228 and 665 cm^{-1}.[23–25] After reacting these beads with vanadyl sulfate a band at 964 cm^{-1} corresponding to the vanadyl ν(V═O) stretch appeared (Fig. 6).[26] The total vanadium content was quantified by using ICP-OES according to a previously used method[22] and found to be 2.80%, giving an imidazole/vanadium ratio of close to 4 : 1.

Investigation of the surface chemistry of these beads by XPS also confirmed the presence of vanadium, along with the other expected elements. The V $2p_{3/2}$ peak appeared at a binding

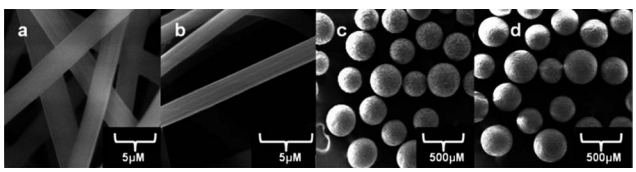

Fig. 4 Selected scanning electron micrographs of (a) p(ST-*co*-VIM); (b) p(ST-*co*-VIM)-VO; (c) p(VIM-*co*-EGDMA) and (d) p(VIM-*co*-EGDMA)-VO.

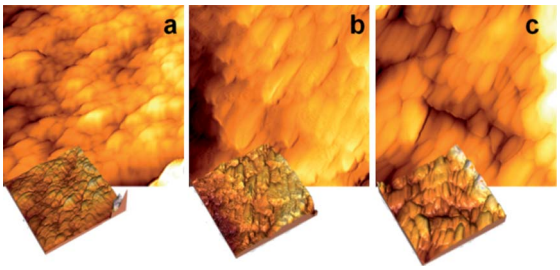

Fig. 5 Selected 2D and 3D (1 × 1 μm sections) of (a) p(VIM-*co*-EGDMA), (b) p(VIM-*co*-EGDMA)-VO and (c) p(VIM-*co*-EGDMA)-VO after one catalytic cycle.

energy of 515.3 eV, which confirms the +4 oxidation state of vanadium (Fig. 7).[27] The BET surface area of the p(VIM-*co*-EGDMA) beads was found to be 151 $m^2\ g^{-1}$, while the average pore volume and diameter was 0.31 $cm^3\ g^{-1}$ and 82 Å, respectively. This surface area was quite similar to the poly(vinylimidazole-*co*-ethyleneglycol dimethacrylate) beads prepared by Kara *et al.*, who reported a surface area of 59.8 $m^2\ g^{-1}$ for their 150–200 μm sized beads.[25] The slightly higher surface area observed in this study may be due to the larger amount of crosslinker used, since it has been shown that an increase in crosslinker may result in greater surface areas.[28] After reaction with vanadyl sulfate, the surface area dropped to 99 $m^2\ g^{-1}$, while the average pore volume and size remained relatively similar (0.21 $cm^3\ g^{-1}$ and 87 Å, pore volume and pore size respectively). The drop in surface area going from p(VIM-*co*-EGDMA) to p(VIM-*co*-EGDMA)-VO may be due to filling of the pores by vanadium, as evidenced by the slight drop in pore volume (BJH), as well as the decrease in surface roughness as measured by AFM.

3.2 Synthesis and characterization of poly(ST-*co*-VIM) fibers

While electrospun fibers may be an attractive option as a catalyst support, there remain certain challenges with this material, especially considering that one is limited to using non-crosslinked polymers when electrospinning. This subsequently affects the choice of solvent to be used in the catalyzed reactions. The

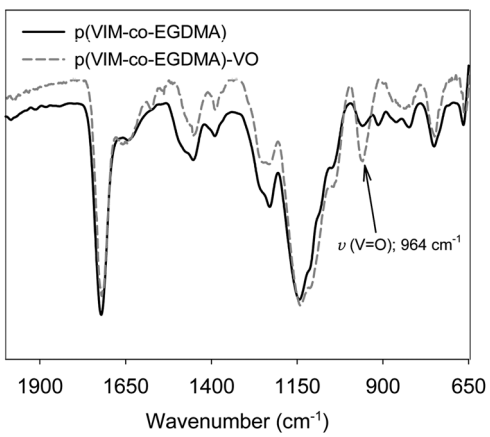

Fig. 6 Infrared spectra of p(VIM-*co*-EGDMA) and p(VIM-*co*-EGDMA)-VO beads. The ν(V═O) has been highlighted.

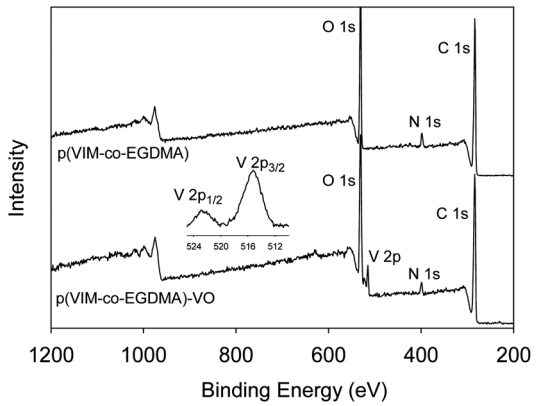

Fig. 7 Wide scan XPS spectra of p(VIM-*co*-EGDMA) (top) and p(VIM-*co*-EGDMA)-VO (bottom). The insert shows the expanded V $2p_{3/2}$ and V $2p_{1/2}$ signals.

homopolymer of N-vinylimidazole for example, is soluble in several solvents and hence unsuitable for this work.[29] For this reason, we prepared styrene-vinylimidazole copolymers. These copolymer fibers unfortunately became tacky and lost the fibrous morphology when placed in acetonitrile. Thus, subsequent catalyzed reactions were performed in methanol rather than acetonitrile, despite the fact that acetonitrile has proven to be a promising solvent for sulfoxidation reactions.[30,31]

The imidazole containing copolymers were prepared by bulk polymerization. A few different ratios of the styrene/vinylimidazole monomers were used. However, besides the imidazole content in the resultant copolymer there was no dramatic effect on solubility or other properties of the fibers, and as such only one ratio was thoroughly studied. Characterization and brief catalysis results of the fibers produced using different monomer ratios may however be found in the supplementary material section.

Based on the elemental composition, the styrene/imidazole content for the p(ST-*co*-VIM) copolymer was approximately 10 : 1. This ratio provided sufficient functionality as well as the required solubility parameters for electrospinning. In the first attempt to prepare the pre-electrospinning functionalized oxovanadium-immobilized polymer, the copolymer was dissolved in DMF and reacted with $VOSO_4$. This reaction produced a green solid which was insoluble in several solvents and therefore could not be electrospun.

Thus, the styrene-imidazole copolymer was first dissolved in a DMF/THF solvent mixture and electrospun into fibers and post-electrospinning introduction of vanadium was carried out. As shown in the SEM images (Fig. 4), the fibers produced were smooth and non-beaded with diameters ranging from 1.3–2.1 μm. Although these diameters are quite large for electrospun fibers, they are still two orders of magnitude smaller than the beads (~300 μm). The imidazole-containing fibers were then immersed in a methanolic vanadyl sulfate solution and stirred for 72 h to produce the oxovanadium(IV)-immobilized fibers. Encouragingly, the morphology of the fibers was unaffected by the reaction with vanadium as witnessed in the SEM images. Much like the microspheres, the average diameter of the fibers increased slightly after the reaction with vanadyl sulfate (1.6–2.4 μm). The BET surface area of the p(ST-*co*-VIM) fibers was found to be 53 $m^2\ g^{-1}$, significantly less than the beads (151 $m^2\ g^{-1}$) despite the smaller diameter of the fibers. This could possibly be attributed to the significantly rougher surface of the beads compared to the fibers as well as the more porous structure of the beads. The pore volume and pore diameter of the unfunctionalized fibers was 0.49 $cm^3\ g^{-1}$ and 309 Å respectively. In this instance, functionalization of these fibers with vanadium resulted in an increase in surface area to 74 $m^2\ g^{-1}$ whilst the pore volume and diameter was 0.67 $cm^3\ g^{-1}$ and 344 Å, respectively. This change may be due to removal of electrospinning solvent after immersion in methanol (during the vanadium functionalization step), thereby producing pores. Elemental characterization data revealed an imidazole-to-vanadium ratio of close to 1 : 1 – a notably different ratio to that observed for the microspheres (4 : 1). Furthermore, the infrared (Fig. 8) and XPS spectra (Fig. 9) suggest the formation a vanadium species in a slightly different coordination environment compared to the beads. For example, the ν(V=O) stretch for vanadyl functionalized fibers appeared at around 980 cm^{-1} compared to 964 cm^{-1} for the microspheres, while the V$2p_{3/2}$ binding energy appeared at 514.9 eV for the fibers compared to 515.3 eV for the beads.

3.3 Catalytic activity

The catalytic activity of the vanadium functionalized beads and fibers was evaluated using different reactor set-ups due to the different properties of the materials. The comparatively larger crosslinked microspheres were more robust compared to the fibers and thus the preferred method of application of the beads was the common batch-type reaction which relies on the agitation of a magnetic stirrer. On the other hand, the polystyrene-based fibers were delicate and susceptible to breaking upon agitation. But the mat-like structure of these materials proved ideal for application in a continuous flow type process.

The reaction used to test the efficacy of both catalytic materials was the hydrogen peroxide facilitated oxidation of thioanisole (Fig. 10).[22,32] This reaction has proven to be a useful indicator for determination of oxidative catalytic activity.[7,22,32,33] Furthermore, the oxidation of sulfides has become a reaction of significant importance since sulfoxides, one of the products of sulfide oxidation, are commonly used as intermediates in the synthesis

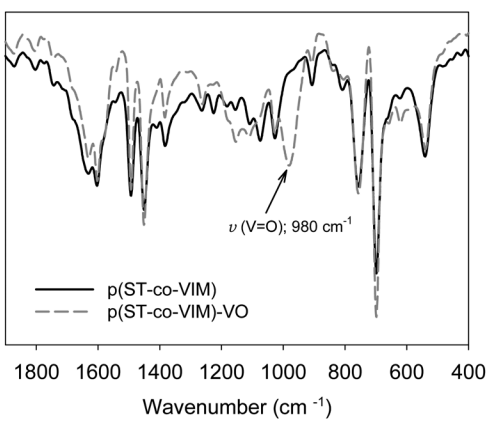

Fig. 8 Infrared spectra of p(ST-*co*-VIM) fiber and p(ST-*co*-VIM)-VO fibers. The ν(V=O) has been highlighted.

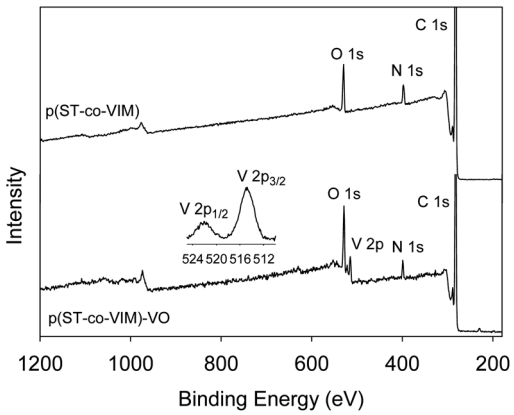

Fig. 9 Wide scan XPS spectra of p(ST-*co*-VIM) (top) and p(ST-*co*-VIM)-VO (bottom). The insert shows the expanded V $2p_{3/2}$ and V $2p_{1/2}$ signals.

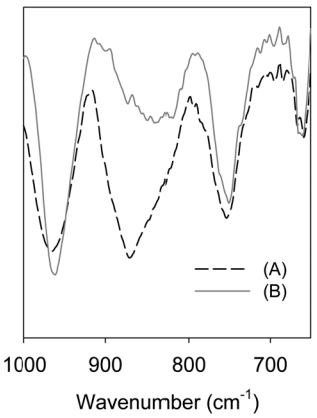

Fig. 11 Overlayed infrared spectra of (A) p(VIM-*co*-EGDMA)-VO and (B) p(VIM-*co*-EGDMA)-VO recovered mid-reaction.

of biologically active compounds. Additionally, oxidative desulfurization, a process used to remove sulfur from fuels, has received a renewed interest due to the current demands for low-sulfur fuels. As shown in Fig. 10, methyl phenyl sulfide may be oxidized to methyl phenyl sulfoxide which is subsequently oxidized to methyl phenyl sulfone. The catalytic mechanism of oxidation by vanadium compounds has been thoroughly studied[34] and a simplified mechanism has been included (Fig. 10). During the catalytic reaction, oxovanadium(IV) is oxidised to dioxovanadium(V) and then oxoperoxovanadium(V). The change in oxidation state is evident from significant change in colour. As shown in Fig. 10, the p-(VIM-*co*-EGDMA)-VO beads turn from a grey-blue colour to a yellow-orange colour, indicative of the change in oxidation state from +4 to +5 as proposed in the mechanism. In the infrared spectrum (Fig. 11), the yellow-coloured beads display a strong band at 966 cm^{-1} consistent with the presence of a terminally bonded V=O group, while the band appearing at 870 cm^{-1} is tentatively assigned the peroxo O–O stretch, ν(O–O).[35] It is therefore likely that the yellow-coloured beads consist predominantly of the oxoperoxovanadium(V) species as would be expected in conditions of excess peroxide.

3.3.1 Catalytic activity of the oxovanadium(IV)-containing microspheres. The first parameter that was optimized was the quantity of catalyst (Fig. 12). As expected, this had a noticeable effect on the rate of oxidation of thioanisole. When using 0.1, 0.2 and 0.3 g of catalyst the TOF's were 34.52, 35.69, 30.12 h^{-1} respectively. For this reason further studies were performed using 0.2 g of catalyst. It should be noted that in the absence of a catalyst a conversion of less than 10% was obtained reinforcing the catalytic properties of the oxovanadium-containing beads. At room temperature, all catalyst quantities gave greater yields of the sulfoxide than the sulfone, but as the quantity of catalyst increased and the reaction time progressed, the ratio of sulfoxide to sulfone began to decrease.

As has been observed before,[22] an increase in temperature resulted not only in an increased rate of oxidation (Fig. 13) but also a greater yield of methyl phenyl sulfone (Fig. 14). At 50 °C, there was a sharp increase in the formation of methyl phenyl sulfoxide, followed by a period of decay with an associated increase in the formation of the sulfone. For the same mass of catalyst, the TOF increased from 35.69 h^{-1} at 25 °C to 268.53 h^{-1} at 50 °C, while the conversions to the sulfoxide were 59.6% (at 25 °C) and 31.2% (at 50 °C), and to the sulfone were 40.2% (at 25 °C) and 68.7% (at 50 °C).

An important property and huge advantage of heterogeneous catalysts over homogeneous catalysts is their ability to be easily

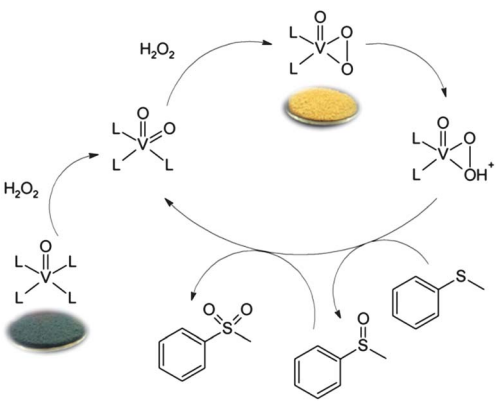

Fig. 10 The proposed catalytic mechanism for the oxidation of thioanisole by vanadium including photographs of beads before and during a reaction.

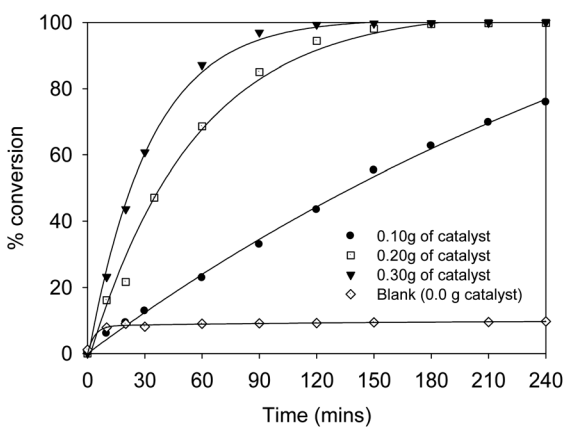

Fig. 12 Effect of amount of using p(VIM-*co*-EGDMA)-VO. Conditions: 20 mmol H_2O_2, 10 mmol thioanisole, 20 ml acetonitrile, 25 °C.

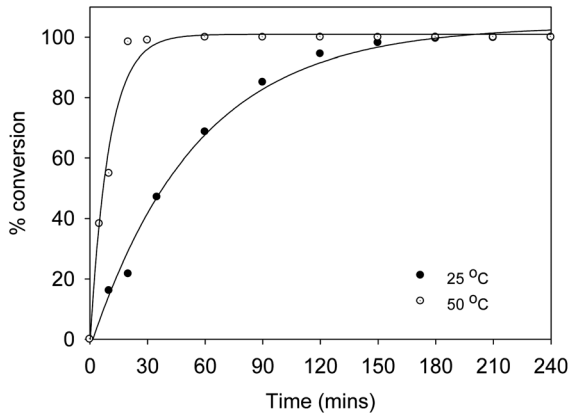

Fig. 13 Effect of temperature using p(VIM-*co*-EGDMA)-VO. Conditions: 0.20 g of catalyst, 20 mmol H_2O_2, 10 mmol thioanisole, 20 ml acetonitrile.

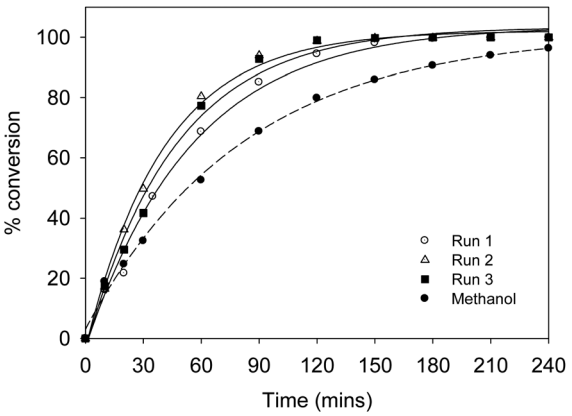

Fig. 15 Recyclability of p(VIM-*co*-EGDMA)-VO beads at optimal conditions and solvent effect. Conditions: 0.20 g of catalyst, 20 mmol H_2O_2, 10 mmol thioanisole, 20 ml solvent, 25 °C.

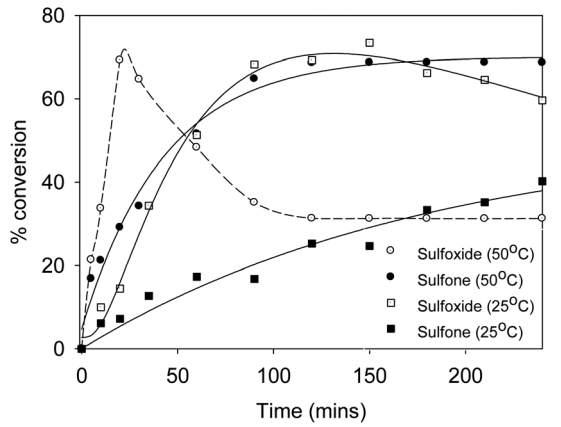

Fig. 14 Effect of temperature on product selectivity using p(VIM-*co*-EGDMA)-VO. Conditions: 0.20 g of catalyst, 20 mmol H_2O_2, 10 mmol thioanisole, 20 ml acetonitrile.

separated and recycled. As shown in Fig. 15 there was barely any drop in activity after successive catalyzed reactions demonstrating the excellent recyclability of these beads. Since the fibers could not be used in acetonitrile, the effect of substituting acetonitrile with methanol was investigated for the beads. As shown in Fig. 15, substitution with methanol results in a slight drop in activity. One proposed explanation for this effect involves the stabilization of the vanadium species by coordination of acetonitrile[36] while another possibility may be due to the slightly higher dielectric constant of acetonitrile (37.5) compared to methanol (33). A summary of the results obtained using p(VIM-*co*-EGDMA)-VO appears in Table 1.

3.3.2 Catalytic activity of the oxovanadium(IV)-containing fibers. As mentioned earlier, for a polymer to be electrospun, it must be soluble or form a melt. This consequently means that the resultant fibers will be soluble in the same solvents unless some sort of post-electrospinning cross-linking strategy is utilized.[37,38] For this reason methanol was selected as the solvent to be used in the fiber catalyzed reactions since methanol did not dissolve or change the fiber morphology in any way. When placed in acetonitrile, however, the fibers lost structural integrity. As demonstrated with the microspherical beads, methanol was not an ideal solvent for this reaction, and so this solvent choice was governed by solubility constraints.

The vanadium-immobilized fibers were used in a continuous flow process, rather than a batch process for reasons discussed earlier. The continuous flow approach also offered certain advantages over the batch process, for example, no catalyst separation was necessary and very little damage to the support material was observed due to the absence of mechanical agitation. The reactant solution was passed through the packed porous fiber mat and the product fractions were collected in 1 ml portions and analyzed by GC (see Fig. 3).

The effect of the amount of catalyst packed into the syringe was first investigated (Fig. 16). It was only at very low catalyst amounts (0.005 g) that any drop in activity was observed over the period studied. This drop in activity may have been due to leaching of the vanadium from the fibrous support material which would have had a more pronounced effect when using lower catalyst amounts – the leaching behaviour was studied and shall be discussed later. Another possibility for the drop in activity may be due to saturation of the catalytic sites.

Besides catalyst amount, another important parameter to be considered when conducting continuous flow reactions is the flow rate – the speed at which the reactant solution was passed through the catalyst bed. This was, in our case, carefully controlled using a syringe pump. As shown in Fig. 17, the flow rate was varied between 1 ml h^{-1} and 6 ml h^{-1}. When higher flow rates were used there was less time was available for the reactant solution to interact with the catalyst bed the consequence being a significant drop in activity (Table 2). Furthermore, the selectivity shifted towards the formation of the sulfoxide as the flow rate increased (Table 2). By altering the catalyst amount and flow rate one can begin to shift the selectivity to either the sulfoxide (lower catalyst amounts or higher flow rates) or the sulfone (low flow rate, high catalyst amounts) depending on which product is desired. A table summarizing these results has been included (Table 2).

Since the fiber-based catalysts showed a drop in activity as time progressed (Fig. 16), we found it necessary to quantify the amount of vanadium leached from the fibers. Each 1 ml fraction

Table 1 Summary of the results obtained at different reaction conditions for p(VIM-*co*-EGDMA)-VO as a catalyst

Mass (g)	*T*/°C	Solvent	Sulfoxide (%)	Sulfone (%)	Conversion (%)	TOF (h^{-1})[a]
0.1	25	CH_3CN	59.3	16.6	75.9	34.52
0.2	25	CH_3CN	59.6	40.2	99.9	35.69
0.2[b]	25	CH_3CN	54.9	45	99.9	44.91
0.2[c]	25	CH_3CN	51.4	48.5	99.9	45.00
0.2	50	CH_3CN	31.2	68.7	99.9	268.53
0.2	25	MeOH	72.8	23.4	96.3	21.89
0.3	25	CH_3CN	55.5	44.4	99.9	30.12

[a] Determined as moles of substrate converted/moles of catalyst/time (h). [b] After one cycle. [c] After two cycles.

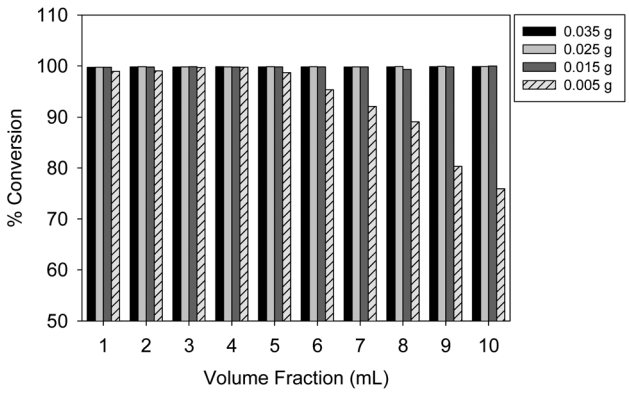

Fig. 16 The effect of the amount of catalyst on overall conversion. Conditions: p(ST-*co*-VIM)-VO, 2 mmol H_2O_2, 1 mmol thioanisole, 10 ml methanol, $\nu = 1$ ml h^{-1}.

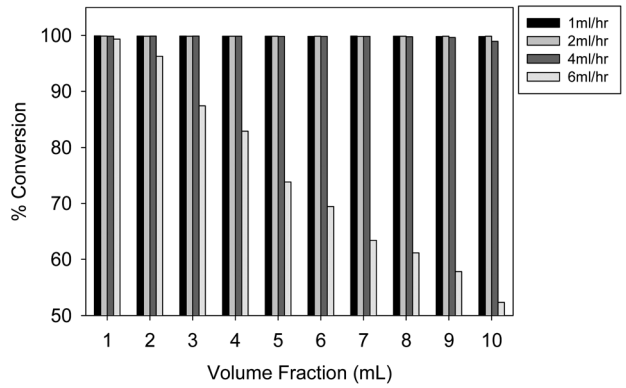

Fig. 17 The effect of flow rate (ν) on overall conversion. Conditions: 0.025 g of p(ST-*co*-VIM)-VO, 2 mmol H_2O_2, 1 mmol thioanisole, 10 ml methanol.

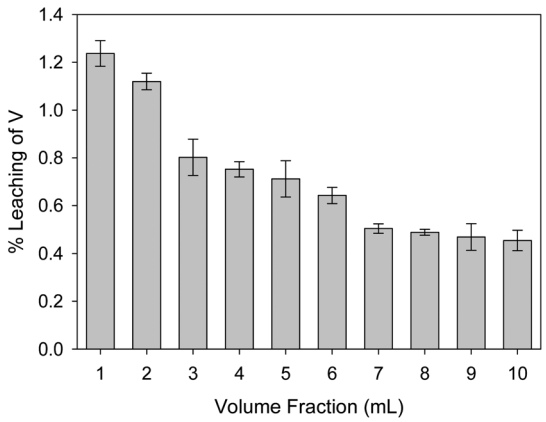

Fig. 18 Vanadium leaching behaviour of p(ST-*co*-VIM)-VO. Conditions: 0.025 g of p(ST-*co*-VIM)-VO, $\nu = 2$ ml h^{-1}, 1 mmol of thioanisole, 2 mmol of H_2O_2, 10 mL methanol (n = 3).

of product solution that was collected was concentrated to remove any organic solvent. After digesting the remaining residue in nitric acid and diluting appropriately, the vanadium content was determined by ICP-OES. In the first fraction about 1.2% (±0.05) of vanadium was detected. This decreased and then stabilized at around about 0.41% (±0.02) (Fig. 18), a similar trend has been observed by others and correlates well to the drop in conversion when using lower catalyst amounts (Fig. 16).[39]

Conclusions

Polymer microspheres containing the imidazole functionality were successfully prepared by suspension polymerization. The corresponding vanadyl-immobilized beads not only successfully

Table 2 Summary of reaction conversions and selectivities for p(ST-*co*-VIM)-VO catalyzed reactions

Mass (g)	Flow Rate (ml h^{-1})	Sulfoxide (%)	Sulfone (%)	Average Conversion (%)[a]
Blank[b]	2	5.98	4.12	10.1
0.005	2	63.8	29.0	92.9
0.015	2	55.6	44.1	99.7
0.035	2	42.7	57.1	99.9
0.025	1	39.7	60.1	99.9
0.025	2	49.0	50.8	99.9
0.025	4	56.1	43.6	99.7
0.025	6	55.7	18.6	74.4

[a] Averaged conversion of 10 × 1 ml fractions. [b] The p(ST-*co*-VIM) fibers (0.025 g) were used as a blank.

catalyzed the oxidation of thioanisole but also proved to be robust and recyclable, showing no drop in activity after three successive cycles. At catalyst amounts greater than 0.1 g, 99.9% conversion of thioanisole was achieved in an acetonitrile solvent. This dropped slightly to 96.3% when using methanol. Poly (styrene-*co*-vinylimidazole) copolymers were successfully electrospun into fibers and functionalized with vanadium. The lower mechanical stability of the fibers rendered them better suited to un-agitated continuous flow conditions, compared to the aforementioned larger, robust microspheres which were suited to stirred-batch conditions. The implication of this was that the catalytic activity and selectivity of the two materials could not easily be compared to one another. Under continuous flow conditions near quantitative conversions were obtained over the time period studied when 0.015 g or more of catalyst was used and the flow rate was less than 6 ml h^{-1}. While these fibrous catalyst supports showed great promise, certain aspects including solubility and mechanical strength require attention before they will be as useful as the crosslinked microspherical counterparts. The imidazole containing microspherical and microfiber materials could in the future be used as generic materials for supporting not only vanadium but also other transition metals for metal-mediated catalysis.

Acknowledgements

We acknowledge the DST/Mintek National Innovation Centre (NIC) at Rhodes University for access to microanalysis, XPS and BET equipment. The authors would like to thank the Electron Microscopy Unit (Rhodes University) for use of the SEM. We are also very grateful for the financial support provided by Sasol and NRF (South Africa).

Notes and references

1 M. J. Clague, N. L. Keder and A. Butler, *Inorg. Chem.*, 1993, **32**, 4754.
2 M. Andersson, A. Willetts and S. Allenmark, *J. Org. Chem.*, 1997, **62**, 8455.
3 H. B. ten Brink, A. Tuynman, H. L. Dekker, W. Hemrika, Y. Izumi, T. Oshiro, H. E. Schoemaker and R. Wever, *Inorg. Chem.*, 1998, **37**, 6780.
4 M. Weyand, H. J. Hecht, M. Kieβ, M. F. Liaud, H. Vilter and D. Schomburg, *J. Mol. Biol.*, 1999, **293**, 595.
5 D. Rehder, *Bioorganic vanadium chemistry*, John Wiley and Sons Ltd., West Sussex, 2008.
6 M. Mba, M. Pontini, S. Lovat, C. Zonta, G. Bernardinelli, P. E. Kündig and G. Licini, *Inorg. Chem.*, 2008, **47**, 8616.
7 M. R. Maurya, A. Arya, A. Kumar and J. C. Pessoa, *Dalton Trans.*, 2009, 2185.
8 M. R. Maurya, M. Kumar and A. Arya, *Catal. Commun.*, 2008, **10**, 187.
9 M. R. Maurya, A. Kumar, M. Ebel and D. Rehder, *Inorg. Chem.*, 2006, **45**, 5924.
10 M. R. Maurya, A. Arya, P. Adao and J. C. Pessoa, *Appl. Catal., A*, 2008, **351**, 239.
11 M. R. Maurya, A. K. Chandrakar and S. Chand, *J. Mol. Catal. A: Chem.*, 2007, **278**, 12.
12 M. R. Maurya, S. Sikarwar and M. Kumar, *Catal. Commun.*, 2007, **8**, 2017.
13 M. M. Miller and D. C. Sherrington, *J. Catal.*, 1995, **152**, 368.
14 R. Ando, T. Yagyu and M. Maeda, *Inorg. Chim. Acta*, 2004, **357**, 2237.
15 K. Ebert, G. Bengtson, R. Just, M. Oehring and D. Fritsch, *Appl. Catal., A*, 2008, **346**, 72.
16 Y. Wang, J. Chen, J. Xiang, H. Li, Y. Shen, X. Gao and Y. Liang, *React. Funct. Polym.*, 2009, **69**, 393.
17 B. Fu, P. Zhao, H.-C. Yu, J.-W. Huang, J. Liu and L.-N. Ji, *Catal. Lett.*, 2009, **127**, 411.
18 Z. M. Huang, Y. Z. Zhang, M. Kotaki and S. Ramakrishna, *Compos. Sci. Technol.*, 2003, **63**, 2223.
19 D. H. Reneker and A. L. Yarin, *Polymer*, 2008, **49**, 2387.
20 J. S. Reichert, S. A. McNeight and H. W. Rudel, *Ind. Eng. Chem.*, 1939, **11**, 194.
21 E. Uguzdogan, E. B. Denkbas, E. Öztürk, S. A. Tuncel and O. S. Kabasakal, *J. Hazard. Mater.*, 2009, **162**, 1073.
22 Z. R. Tshentu, C. Togo and R. S. Walmsley, *J. Mol. Catal. A: Chem.*, 2010, **318**, 30.
23 T. J. Lane, I. Nakagawa, J. L. Walter and A. J. Kandathil, *Inorg. Chem.*, 1962, **1**, 267.
24 C. G. Overberger and N. Vorchheimer, *J. Am. Chem. Soc.*, 1963, **85**, 951.
25 A. Kara, L. Uzun, N. Besirli and A. Denizli, *J. Hazard. Mater.*, 2004, **106**, 93.
26 G. Wilkinson, R. D. Gillard and J. A. McCleverty, *Comprehensive Coordination Chemistry*, Pergamon Press, New York, 1987.
27 C. J. Groenenboom, G. Sawatzky, H. J. de Liefde Meijer and F. Jellinek, *J. Organomet. Chem.*, 1974, **76**, C4.
28 K. C. Gupta, H. K. Abdulkadir and S. Chand, *J. Mol. Catal. A: Chem.*, 2003, **202**, 253.
29 M. ÖzyalçIn and Z. Küçükyavuz, *Synth. Met.*, 1997, **87**, 123.
30 M. Bagherzadeh, R. Latifi, L. Tahsini and M. Amini, *Catal. Commun.*, 2008, **10**, 196.
31 M. Bagherzadeh, M. Amini, D. M. Boghaei, M. M. Najafpour and V. McKee, *Appl. Organomet. Chem.*, 2011, **25**, 559.
32 R. S. Walmsley and Z. R. Tshentu, *S. Afr. J. Chem.*, 2010, **63**, 95.
33 M. R. Maurya, A. K. Chandrakar and S. Chand, *J. Mol. Catal. A: Chem.*, 2007, **274**, 192.
34 M. R. Maurya, A. Arya, A. Kumar, M. L. Kuznetsov, F. Avecilla and P. J. Costa, *Inorg. Chem.*, **49**, p. 6586.
35 N. J. Campbell, A. C. Dengel and W. P. Griffith, *Polyhedron*, 1989, **8**, 1379.
36 Z. Du, J. Ma, H. Ma, M. Wang, Y. Huang and J. Xu, *Catal. Commun.*, 2010, **11**, 732.
37 C. Tang, C. D. Saquing, J. R. Harding and S. A. Khan, *Macromolecules*, 2009, **43**, 630.
38 X. Xu, J.-F. Zhang and Y. Fan, *Biomacromolecules*, 2010, **11**, 2283.
39 M. M. Miller and D. C. Sherrington, *J. Catal.*, 1995, **152**, 377.

